

Assessment of Carotid Artery Vibrations by Using Optical Flow Methods on Ultrasound Images and Optical Flow

Saba Rabiee¹, Parisa Rangraz^{1*} , Ahmad Shalbaf^{2*} 

¹ Department of Biomedical Engineering, Science and Research Branch, Islamic Azad University, Tehran, Iran

² Department of Biomedical Engineering and Medical Physics, School of Medicine, Shahid Beheshti University of Medical Sciences, Tehran, Iran

*Corresponding Authors: Parisa Rangraz, Ahmad Shalbaf
Email: p.rangraz@gmail.com, shalbaf@sbmu.ac.ir

Received: 10 February 2023 / Accepted: 03 July 2023

Abstract

Purpose: This study aims to extract carotid wall vibrations non-invasively and evaluate changes in the carotid artery caused by age, BMI, and sex. Such evaluation can increase the possibility of detecting wall stiffness and atherosclerosis in the early stages and prevent heart attack and death.

Materials and Methods: To extract small vibrations of the carotid wall, the image-tracking method, and optical flow with four different methods were used. The study involved twenty participants, comprising six females and fourteen males, with a mean age of 36.25 years, mean weight of 75.2 Kg, and mean BMI of 25. The posterior wall motion and vibration were extracted using ultrasound RF signals.

Results: 4 optical flow methods, Gunnar-Farneback, Horn-Schunck, Lucas-Kanade, and Lucas-Kanade derivative were used for all samples, and covariance, correlation, P-value, and R-squared were estimated. Results showed the differences in parameters such as age and BMI with carotid wall vibration. These values for age are (Cov = -0.1891, Corr = -0.6770, P-value < 0.001, $r^2 = -0.4590$) and for BMI are (Cov = -0.0564, Corr = -0.6510, P-value < 0.001, $r^2 = 0.4238$), respectively. For gender as a new parameter, a comparison between men's and women's vibrations was estimated. The range of measured vibrations by optical flow methods is about 0.0002 μm to 0.1 μm , and the mean standard deviation is 0.04967 μm .

Conclusion: The results presented that gender affects the vibration of the vessel wall, which in men is more than in women. In addition, increasing age and BMI may increase the stiffness of the carotid wall and reduce vibrations that were evaluated previously. Using the Gunnar-Farneback method as image tracking for small vibrations is the best way with the highest accuracy.

Keywords: Optical Flow; Ultrasound; Image Tracking; Age; Body Mass Index; Radio Frequency Signal.

1. Introduction

Artery wall motions and vibrations are used as a criterion for determining the characteristics of vessel walls. Hence, quantitative evaluation of atherosclerosis is necessary for the early diagnosis of heart diseases [1, 2]. Heart attacks are one of the leading causes of death today. Early diagnosis of clogged arteries and help with timely treatment can eliminate atherosclerosis and increase a person's health and longevity. Therefore, this study was conducted to detect clogging with the help of wall vibrations using the optical flow image tracking method on ultrasound images. B-Mode ultrasound allows non-invasive recording of the arterial wall and plaque movement in radial and longitudinal directions [3-5]. Ultrasound images provide better images than other imaging methods due to the probe being located near the target tissue, which is the carotid artery, and in this method, the wall is well separable. Also, this method is less dangerous and expensive than other methods due to not using x-ray. To examine ultrasound images, we need to investigate them frame by frame. Since the fact that a specialized radiologist is not present in all imaging centers, and due to the tedious time of the frame-by-frame examination, it is necessary to use the image-tracking method to facilitate diagnosis, saving time and money. The optical flow method gives a good approximation of the actual physical vibrations. Because it checks frame by frame, and there is no possibility of losing information. Also, the optical flow provides a brief description of both the region of the image motion area and the motion velocity.

Various methods have been used to study the movements and vibrations of carotid arteries and tissues. In 1993, Hein *et al.* used the time-amplitude method in RF ultrasound signals to evaluate tissue movements. The time-domain method is used to estimate tissue motion. They proved that this method has many advantages over the Doppler method used in the past. One of the advantages of this method for estimating blood flow velocity is that selecting which pair of echoes are used to calculate the estimate for a given pulse repetition period can optimize the accuracy of velocity estimation [3]. Several studies have been conducted to evaluate different methods for calculating optical flow and to improve the accuracy of carotid artery wall vibration detection. Local and global methods have been used, but no clear attempt has been made to combine their benefits in previous

studies. Researchers have proposed various methods, such as dense flow fields that are resistant to noise and the separation of wall signals from blood signals. Some studies have focused on estimating the velocity of ultrasound image sequences, while others have evaluated new, non-invasive techniques for tracking the radial and longitudinal movements of the artery wall. The Optical flow method has been used to evaluate the motion of the carotid artery wall, but there are limitations due to reliability issues in image data acquisition. Additionally, several studies have investigated the effect of aging and overweight on carotid arterial wall vibrations. These studies are important for combining different methods and examining gender differences [4-12].

From 2011 to 2018, Zahnd *et al.* presented various divisions of methods for determining arterial movement. In 2011, their study was conducted on two different groups (26 older diabetic patients and 26 young healthy volunteers). The goal was to investigate the relationship between risk factors, and the filter response is only optimal for a velocity range (2-D) movement of the arterial wall. To achieve this goal, a spot tracking approach was proposed to estimate the 2-dimensional pathway of the vessel wall and applied to the left Common Carotid Artery (CCA) Ultrasound Sequences B (US). A deformable skeleton model was also introduced in the block-matching design [11]. They proposed a multi-block matching method for evaluating multiple blocks simultaneously, which yielded reliable results. This method evaluates the longitudinal and radial motion of clinical B-mode ultrasound sequences in-vivo. To estimate the path of a selected point during the cardiac cycle, they introduce a block-matching method that involves temporarily updating the reference block using a pixel-based Kalman filter [12]. Also, they devoted a study to introduce a real-time beamforming strategy that captures images labeled with a distinct pattern on the target for ease of tracking. They used the LPBOF estimator to study the Optical flow method [13]. They have a study on longitudinal kinetics. The vast majority of (semi-automated) methods developed to measure this so-called "longitudinal kinetics" are based on point tracking, so they cannot record the total and potentially heterogeneous motion of the entire artery wall. The purpose of this work is to introduce a motion-tracking framework that can simultaneously extract the time path of a large set of points (several hundred) that are horizontally aligned and cover the entire usable width of the image, so it creates a dense motion field [14]. Yousefi *et al.* [15] presented a method to evaluate the

effect of aging on Carotid arterial wall vibrations by using experimental model analysis. The method, which uses a phase tracking method based on continuous wavelet conversion, calculates the movement of the carotid wall from ultrasound radio frequency signals. Then, it was used to extract high-frequency components of wall motion, wall vibration, and experimental mode analysis. In this study, the effect of aging and overweight on the dominant frequency of vibration and peak-to-peak amplitude is considered. In the study, about 35 to 40 cases were studied, which were compared with similar cases, and this method is important by combining the two methods and examining gender.

Several studies have been conducted to evaluate different methods for calculating optical flow and to improve the accuracy of carotid artery wall vibration detection. Local and global methods have been used, but no clear attempt has been made.

Golemati *et al.* have a study on spackle tracking and modeling, used to calculate texture displacement from a sequence of images. Then, Kinematic and mechanical indicators are extracted from it. These shifts can provide valuable functional information about the cardiovascular system under normal conditions and disease. Using the low spatial resolution of B-mode images, a hybrid scheme is proposed in which large displacement estimates are obtained from B-mode images, and RF data is used to guide high-resolution estimates [16]. In 2017, Chuang *et al.* used the advantages of optical flow and adaptive block-matching methods to study tendon movements. Initially, the study used the optical flow method to analyze two pairs of adjacent frames, followed by the application of Multiple Kernel Block-Matching (MKBM) methods to spaced frames. While the optical flow method can accurately track and evaluate target vibrations with small amounts of motion, it may fail when the target motion is too large. On the other hand, the MKBM method can track target movement between large time intervals but may perform poorly when target motion is too small. The study aims to use the optical flow method to obtain vibrations between consecutive frames and investigate the degree of artery blockage for early diagnosis and prevention of fatal outcomes. The study improves upon previous research by simultaneously utilizing several optical flow methods to achieve the most precise results [17]. This study aims to utilize the optical flow method to obtain vibrations between consecutive frames for investigating the extent of artery blockage, facilitating early diagnosis, and

preventing fatalities. The study is unique in its use of multiple optical flow methods simultaneously, thereby achieving the most accurate results compared to previous research. The Gunner-Farneback, Horn-Schunck, Lukas-Kanade, and Lukas-Kanade derivatives of Gaussian are different optical flow methods, which may be implemented for all participants. Moreover, it is important to take into consideration the potential impact of age, weight, and sex. Previous studies have overlooked the role of gender, but this particular study seeks to examine novel connections between sex and carotid wall vibrations.

2. Materials and Methods

2.1. Study Design

In this study, we used the MyLab60 ultrasound system (manufactured by Esaote) equipped with a LA532 linear array probe at a frame rate of 60 frames/s, by B-mode, which is connected to a PC for preprocessing. The central frequency is 13 MHz and the sampling frequency is around 20 MHz regardless of the dead time. Each record contains 360 frames, which is roughly equivalent to six cardiac cycles and is scanned radially from the left common carotid artery. RF signals were recorded and converted into data matrices using MATLAB2015b software. These matrices have average dimensions of $360 \times 129 \times 2526$. The number of sample points in the depth direction is 2526, the number of RF lines is 129, and the number of frames is 360, which is recorded in 6 seconds for each sample. In this study, we tried not to examine the domain with this method and the pixel was evaluated with pixels and intensity, and the color was avoided. The conditions for receiving signals from individuals have been as uniform as possible like environmental conditions of the laboratory, such as light, temperature, and sound, which may affect the result, and try to use the same people as much as possible in conditions like sleep, food, and stress. A total of thirty individuals with varying ages, weights, and genders were randomly selected, but only twenty met the criteria for the study. Data was collected in a university laboratory under the guidance of a specialist, and all participants were provided with detailed information regarding the procedures and ultrasound technology (Table 1).

Table 1. The mean age and BMI for 20 volunteers are shown below. Covariance, Correlation, P-value, and r-squared are calculated as a criterion for evaluation

	AGE	BMI
MEAN	36.25 years	25(75.2 Kg for weight)
COVARIANCE	-0.1891	-0.0564
CORRELATION	-0.6770	-0.6510
P-VALUE	< 0.001	< 0.001
R-SQUARED	-0.4590	0.4238

RF signals were generated in MATLAB to analyze the motions and vibrations of the artery wall. An ultrasound device was used to capture the signals, which were then processed and converted into an image using MATLAB software. Ultrasound was preferred over MRI for instant diagnosis as it allowed for the detection of large amplitude vibrations caused by heartbeats. However, ultrasound has limited resolution in detecting small movements. To overcome this, a combination of two methods was used to analyze both large and small movements. The study also evaluated the impact of gender, which was a novel addition to previous methods.

2.2. Optical Flow Technique

Optical flow is one of the image tracking methods in which a change in light I roughly equivalent to the six cardiac cycles and the method is used to measure small

vibrations of consecutive frames. Optical flow is defined as the apparent motion of individual pixels on the image plane as shown in Figure 1a [18]. Most methods that compute optical flow assume that the color/intensity of a pixel is invariant from one video frame to the next. The calculation of light intensity is affected by changes in noise and brightness. Optical flow algorithms estimate the speed and direction of a moving object from one image or video frame to another. Sparse techniques only need to process some pixels from the whole image, but dense techniques process all the pixels. Dense techniques are slower but can be more accurate. Optical flow methods are separated into these two techniques. According to Figure 1b, between consecutive frames, image intensity can be expressed as (I) , displacement, function as (x, y) , and time as (t) . If the first image is $I(x, y, t)$ and its pixels are displaced as (dx, dy) over time t , the new image is $I(x + dx, y + dy, t + dt)$ [19]. First, it is assumed that the pixel intensity of an object is constant between frames (Equation 1) [19].

$$I(x, y, t) = I(x + \delta x, y + \delta y, t + \delta t) \tag{1}$$

The Taylor RHS series approximation is then used and common expressions are omitted (Equation 2) [9].

$$I(x + \delta x, y + \delta y, t + \delta t) = I(x, y, t) + \frac{\partial I}{\partial x} \delta x + \frac{\partial I}{\partial y} \delta y + \frac{\partial I}{\partial t} \delta t + \dots \rightarrow \frac{\partial I}{\partial x} \delta x + \frac{\partial I}{\partial y} \delta y + \frac{\partial I}{\partial t} \delta t = 0 \tag{2}$$

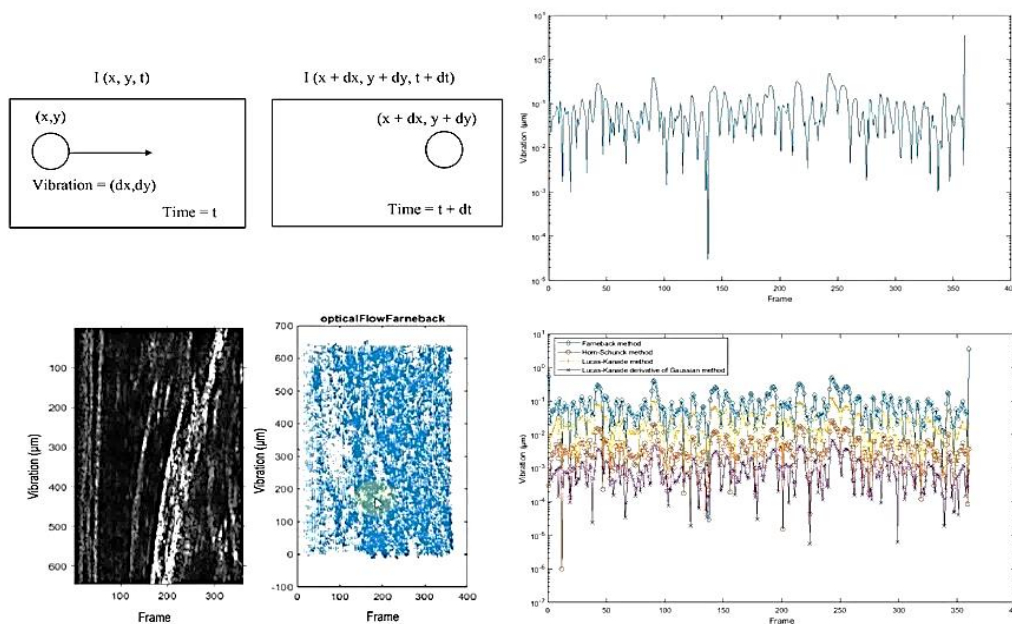


Figure 1. a) Definition of optical flow in mathematical language, b) Gunnar-Farneback signal from a vessel wall vibration related to one of the cases, c) An image of vibrations from vessel wall related to one of the samples by Farneback method, d) Four methods of optical flow for a sample.

Now divide by dt to get the optical flow Equation as follows (Equation 3) [9]:

$$\frac{\partial I}{\partial x} \delta v + \frac{\partial I}{\partial y} \delta v + \frac{\partial I}{\partial t} = 0 \quad (3)$$

In the above function $u = \frac{dx}{dt}$ and $v = \frac{dy}{dt}$. Also $\frac{dI}{dt}$, $\frac{dI}{dx}$, and $\frac{dI}{dy}$ are image gradients on the horizontal, vertical, and time axes [18]. It noted that the optical flow equation for u and v could be solved directly because there is only one equation for two variables. Therefore, different methods are used to solve optical flow problems. In the following, we may explain the methods.

There are four methods to detect movement in video images: GF, HS, LK, and LK-DOG. GF estimates motion using quadratic polynomials, HS uses a quadratic term of smoothness, LK registers images using spatial intensity gradient, and LK-DOG estimates the direction and speed of moving objects by adding excessive interpolation levels.

2.3. Validation of Analysis

In descriptive statistics, a box plot graphically represents local groups, the breadth, and the skewness of numerical data through their quartiles. In addition, lines (called mustaches) in the box diagram indicate variability outside the upper and lower quarters. Hence, the design is also referred to as the box-and-whisker plot. Box plots are non-parametric: they show variability in samples of a statistical population without any assumptions about the underlying statistical distribution. The spacing in each sub-section of the box plot indicates the degree of dispersion and skewed, which is usually described using a five-number summary.

The p-value is a statistical indicator that indicates the likelihood of obtaining test results that are equal to or greater than the observed results, given that the null hypothesis is valid. A low p-value suggests that the observed result is unlikely to have occurred by chance under the null hypothesis.

For most tests, the null hypothesis is that there is no relationship between your favorite variables or that there is no difference between the groups. R-squared is a statistical measure that shows the ratio of the variance of a dependent variable as explained by an independent variable or variables in a regression model. Although correlation measures the relationship between two variables, R-squared indicates the proportion of variance

in one variable that can be explained by another variable. If R-squared is 100%, it means that the movements of one variable completely account for the movements of the other variable. In this study, we propose the following model.

3. Results

Different methods at different ages, weights, and genders have been shown. The outcomes of methods show that the vibrations are in the range of a few tenths to a few thousandths of a micrometer and are near to reality. The vibrations were calculated frame by frame in each cardiac cycle and averaged. In age, the optical flow algorithms investigated the carotid wall vibrations in two different age groups. Vibrations for 20 cases of different ages with various methods are presented in Figure 2a-2d. The maximum amount, which is the highest data value, is slightly higher in the young group than in the middle-aged group and is about $0.0004 \mu m$ at the highest point. The minimum is in the same young group and is at the lowest point, about $0.0001 \mu m$. The red line, which shows average vibration, in the young group is about $0.00021 \mu m$ and it is higher than the middle-aged (40 years) group, which is about $0.05075 \mu m$. This shows that the vibrations in young people in the GF method are more than middle-aged. In the young group, the variability in the upper quarter is more than middle-aged and it is about $0.00018 \mu m$. As shown in Figure 2a. In the HS method, which is explained in Figure 2b, the maximum in the young group is higher than the middle-aged and is at the highest point around $0.00125 \mu m$. Also, the reported vibration quantities are not proved by other

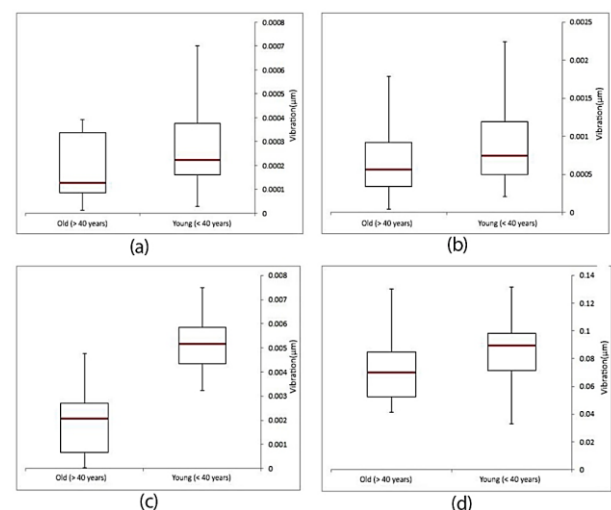


Figure 2. Box plot for two age groups of young (less than 40 years) and middle-aged (more than 40 years)

methods, and the reported values by various optical flow methods are more than 100 percent different from each other. The minimum is in the middle-aged group and at the lowest point is about $0.0004 \mu m$. The red line, which shows average vibration, is about $0.0075 \mu m$ and is higher than the middle-aged one, which is about $0.005 \mu m$; therefore, the vibration in youth is higher than in the middle-aged. In the young group, the variability in the upper quarter is more than middle-aged and it is about $0.0005 \mu m$. In the LK method, the maximum in the young group is more than in the middle-aged group and is about $0.006 \mu m$ at the highest point. The minimum is related to the middle-aged group and at the lowest point is about $0.001 \mu m$. In the young group, the variability in the upper quarter is more than in middle-aged and it is about $0.0045 \mu m$. The red line, in the young group, is about $0.0052 \mu m$ and it is higher than the middle-aged (40 years) group with $0.002 \mu m$ vibrations as shown in Figure 2c. The maximum in the LKDOG in the young group is higher than in the middle-aged group and at the highest point is about $0.1 \mu m$. This discrepancy in the data may be due to the presence of one or more outliers. The minimum is in the middle-aged group and is at the lowest point of about $0.0001 \mu m$. The red line, in the young group, is about $0.06 \mu m$ and it is higher than the middle-aged (40 years) group. In the young group, the variability in the upper quarter is more than middle-aged and it is about $0.07 \mu m$. The average vibration with the red line in the youth group is about $0.09 \mu m$ more than the middle-aged group which is about $0.07 \mu m$ as shown in Figure 2d. In BMI, after computing the effects of age in different methods, we examine the effects of weight in two different categories: normal weight ($BMI < 25$) and overweight ($BMI > 25$). In the GF method, the maximum amount is higher in people with a $BMI < 25$ than in people with $BMI > 25$ and at the highest point, it is about $0.00045 \mu m$. The minimum, which is the lowest amount in the $BMI > 25$, is at the lowest point about $0.0002 \mu m$. Also, in the $BMI < 25$ group, the variability in the upper quarter is about $0.00019 \mu m$ and it is approximately the same as $BMI > 25$ group. The red line, which shows average vibration, in the $BMI > 25$ is about $0.00029 \mu m$ and it is higher than the $BMI < 25$ group, which is about $0.05075 \mu m$. Figure 3a shows the relationship between vibration and BMI in the HS method.

The maximum amount in the $BMI < 25$ group is higher than in the group with $BMI > 25$ and at the highest point, it is about $0.0013 \mu m$. The minimum in the same group is $BMI > 25$ and is at around $0.0004 \mu m$. Also, the

average vibrations in the group of people with $BMI < 25$ is about $0.0075 \mu m$ and is higher than the group of people with $BMI > 25$, which is about $0.0005 \mu m$, and this shows that the vibrations in the first group are more than the second group. The relationship between the two groups in the LK method showed in Figure 3c. The average BMI in people with normal weight is higher than overweight. The maximum amount in people with a $BMI < 25$ is higher than in people with a $BMI > 25$ and at the highest point is about $0.006 \mu m$ and the minimum in the $BMI > 25$ group is at the lowest point and about $0.0025 \mu m$. Also, the average vibrations shown by the red line, in the group of people with $BMI < 25$ is about $0.005 \mu m$ and is higher than the group of people with $BMI > 25$ which is about $0.004 \mu m$, and this shows that the vibrations in the first group are more than the second group. In the LKDOG method, the highest point is about $0.00045 \mu m$. The minimum is in the $BMI < 25$ group and is at the lowest point of about $0.0002 \mu m$. Also, the average vibration in the group of people with $BMI < 25$ is about $0.0003 \mu m$ and more than the group of people with $BMI > 25$ which is about $0.0002 \mu m$ Figure 3d.

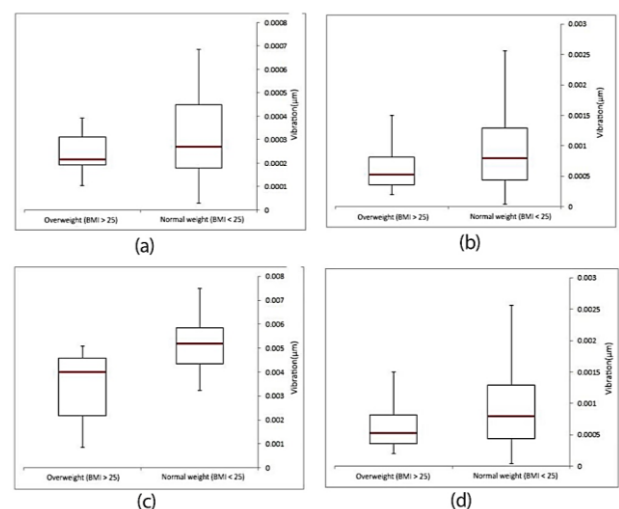


Figure 3. Box plot for wall vibrations in overweight people ($BMI > 25$) compared to normal-weight people ($BMI < 25$)

The purpose of considering age and weight equally was to eliminate their effect on vibrations and investigate sex effects on carotid wall vibrations. Figure 4a is drawn for the two data sets, male and female. A similar age group with similar weights and equal numbers of men and women (age group of 23-year-olds weighing about 75 Kg) was selected and the effect of gender on them was shown. The relationship between vibration and gender in two different groups by the GF method shows that vibrations in men are more than in women. The maximum, which is

the highest data value, is in the male group and is about $0.04 \mu\text{m}$ at the highest point. The minimum, which is the lowest value, is in the same group of men and is at the lowest point, about $0.012 \mu\text{m}$. The average vibration that is shown by the red line, in men is about $0.025 \mu\text{m}$ which is higher than the average vibration in women, and it is about $0.018 \mu\text{m}$. The relationship between vibration and gender in men and women in the HS method shows that the maximum is in the male and it is about $0.0015 \mu\text{m}$ at the highest point. The minimum is related to women and it is about $0.0002 \mu\text{m}$. In addition, the average vibration in men is about $0.001 \mu\text{m}$, which is higher than the average vibration in women, which is shown in Figure 4b. Figure 4c, by using the LK method, proves that vibrations in men are higher than in women. The maximum is in the male group and it is about $0.007 \mu\text{m}$ at the highest point and the minimum is in the female group and at the lowest point is about $0.0035 \mu\text{m}$. In addition, the average vibration in men is about $0.006 \mu\text{m}$, which is higher than the average vibration in women, which is about $0.004 \mu\text{m}$ at the highest point. In the LKDOG method, the maximum is in the male group and is about $0.0003 \mu\text{m}$ and the minimum is related to women which is about $0.0001 \mu\text{m}$. The average vibration in men is about $0.00023 \mu\text{m}$, which is higher than the average vibration in women, which is about $0.00015 \mu\text{m}$ in Figure 4d.

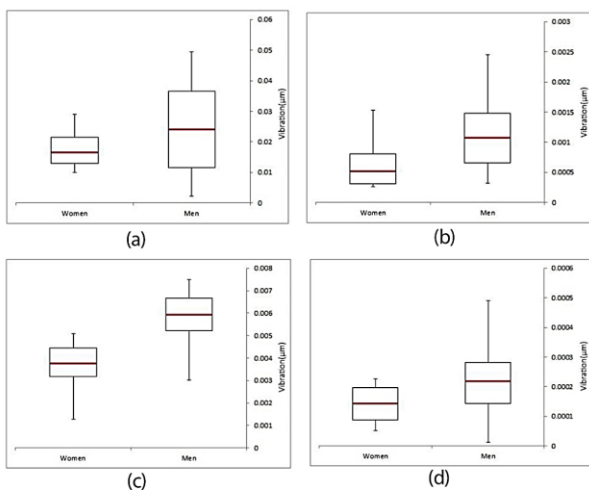


Figure 4. Box plot for wall vibrations in men and women

Comparing optical flow methods with each other shows that the Horn-Schunck estimation method yields high-density flows but is more sensitive to noise than other methods. The GF and LK algorithms have better performance for simple block matching in terms of time. The HS algorithm takes high computational time because of repetitions and thus resulting in mathematical

complexity. This can be modified in the LK algorithm by implementing the Least Square method.

The study compared LK and GF optical flow methods for detecting carotid wall vibrations, with GF showing higher accuracy. LK is better for detecting interesting points while LKDOG is more robust to noise. Men generally had higher vibrations than women, with weight and age also affecting results.

4. Discussion

The study methodology involved asking participants to remain in a resting state while RF signals were recorded by placing a probe on the carotid artery. Frame-by-frame vibrations were then recorded using four optical flow methods (GF, HS, LK, and LKDOG), and the mean of vibrations was calculated for each participant. These results were compared and recorded in Table 2 based on age, BMI, and gender. Finally, standard deviation, covariance, correlation, p-value, and R-squared values were obtained to facilitate comparison of the results. The lowest vibration value, obtained in this study is $0.0002387 \mu\text{m}$ related to the Lucas-Kanade derivative of the Gaussian method, and the maximum is $0.131594763 \mu\text{m}$ related to the Gunner-Farneback method. According to obtained results, with aging and weight growth, the hardening of the arterial wall may increase and vibrations in this area may reduce. Gender as a new parameter was investigated in this study and showed that carotid wall vibrations in men are less than in women. Also, if they are in middle age with high weight, the possibility of atherosclerosis may increase greatly. For better comparison, the results of the standard deviation are calculated. A standard deviation is a number that measures how far the data are spread from the mean. The highest standard deviation is for line 18, the Gunner Farneback method is 0.57 and the lowest value is for line 9, the Lucas-Kanade derivative method of the Gaussian method is 0.0002. As mentioned earlier, the closer this value is to zero, the greater the reliability.

There is no absolute winning algorithm, however in general the Gunner-Farneback method performs best. The results of Table 3 show that the Gunner-Farneback algorithm is a useful method in terms of execution time and accuracy to find atherosclerosis in the early stage. The negative gradient of the graph in Figure 5a and 5b indicates that there is a decrease in vibration with increasing age and BMI in both characteristics.

Table 2. The average vibration of each participant in four Optical flow methods

Row	Age	Weight	Sex	GF (µm)	HS (µm)	LK (µm)	LK-DOG (µm)
1	23	75	Male	0.100084828	0.004542496	0.023546702	0.001111581
2	23	70	Male	0.108193362	0.00477958	0.026195292	0.001193369
3	23	69	Female	0.073247207	0.002356881	0.014519063	0.000610715
4	23	68	Male	0.111094763	0.004282456	0.024108413	0.001019886
5	23	75	Female	0.061535893	0.002582929	0.014369332	0.000660708
6	30	70	Male	0.099288262	0.005702556	0.032041573	0.001841076
7	32	66	Male	0.08098792	0.002622528	0.014264286	0.000558069
8	33	75	Male	0.094127297	0.004489778	0.02828119	0.001397885
9	34	63	Male	0.090056622	0.001489892	0.008598752	0.000331999
10	36	76	Male	0.084877304	0.003978763	0.022859652	0.000990179
11	41	94	Male	0.053366846	0.002301814	0.012877087	0.000594242
12	42	60	Male	0.063274109	0.002331092	0.011989855	0.00047108
13	45	90	Male	0.045337602	0.002283561	0.012841436	0.000611072
14	45	60	Male	0.044147697	0.00198144	0.010984418	0.000475902
15	46	80	Male	0.050268618	0.002592479	0.016074002	0.000700065
16	49	75	Female	0.051369363	0.005706748	0.034130356	0.001627749
17	50	104	Male	0.031392946	0.001376724	0.006496993	0.000238669
18	52	75	Male	0.086859056	0.002304908	0.011851755	0.000471342
19	52	69	Male	0.079125054	0.003201114	0.015694378	0.000710234
20	63	83	Female	0.038603571	0.002339755	0.00273296	0.000258907

The main reason for studying the four optical flow methods was to find the best accurate way for factors, affecting carotid wall vibrations. In Table 3, to compare with previous researches, Zahn *et al.* used optical flow as a tracking method in the longitudinal direction. Reported results show a P-value < 0.001 [8]. Yousefi *et al.* used tracking based on the amplitude of vibrations and peak-to-peak distance, which the studied parameters were more

about BMI and age, and the effect of gender did not consider before. Their reports for correlation between age and vibration was -0.5887, for BMI and vibration, was -0.4838 and the p-value was less than 0.001 [10].

Gao *et al.* used a new tracing method based on nonlinear space in the radial direction. The reported p-value was less than 0.001 [2]. Previous studies had

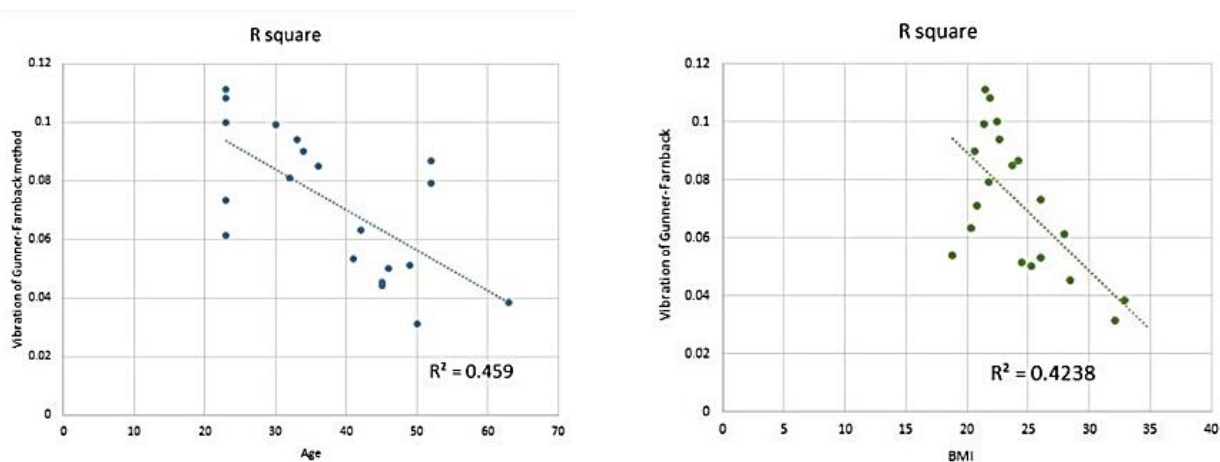


Figure 5. a: The relationship between age and vibration using the Gunner-Farneback method. b: The relations between BMI and vibration using the Gunner-Farneback method

research on age and BMI but other parameters like gender were never considered. Also, in tissue motions, 3 Optical flow methods, GF, HS, and LK were considered but it was the first time that 4 Optical flow methods were deliberated and compared in carotid wall vibrations to find out the best method and results for atherosclerosis prediction.

Table 3. R-squared was calculated for each optical flow method separately in age and BMI

Method	GF	HS	LK	LK- DOG
age	0.459	0.451	0.447	0.453
BMI	0.423	0.0266	0.0927	0.0831

In comparison with other related projects, this study has the same results in the p-value and better results in correlation also presented r-squared and covariance for more emphasis. Moreover, it has a special look at sex as a new parameter, which has not been evaluated before, and its effect on artery wall vibrations. it is possible to observe small vibrations with different methods simultaneously as well. During this, the Gunner-Farneback method has the best results and traces vibrations more accurately. All methods of Optical flow have an overlap between the groups in some places in Figure 2 and Figure 3. In the young group, the variability in the upper quarter is more than middle-aged. Also, the spacing in each sub-section of the middle-aged group box plot is less than the in young group, which investigates the degree of dispersion and skewed. The relationship between vibrations and BMI in two different groups, the average body mass index in normal-weight people is higher than in overweight people. This means that vibrations are higher in people with BMI < 25 than in people with BMI > 25, and as they gain weight, their body

mass index increases, and caused a decrease in vibrations. The volume of data recorded from the carotid artery RF signals is about 10 GB, and by usual computer systems, the ability to read data and processing is faced with memory and is done slowly. Also, access to a limited statistical population makes the project need to be re-examined with a larger number of samples for widespread use [19-24]. In addition to these restrictions, suggestions for future work may be provided. One of the most important practical suggestions is to equip hospitals and imaging clinics with ultrasound devices in this system. With the help of this research, rapid and easy diagnosis of clogged arteries and prevention of subsequent risks can be done non-invasively [25-30]. As well as, examining the effects of lifestyle, exercise, genetics, and nutrition compared to other people who do not exercise or act poorly, may have different results. In addition to the method used in this project, the Optical flow, other image tracking methods such as adaptive block matching can be used simultaneously or separately to evaluate larger movements of the vessel wall.

5. Conclusion

This non-invasive study aims to improve optical flow methods by using image tracking to more accurately evaluate carotid wall vibrations and detect early signs of wall stiffness and atherosclerosis. The study also investigates whether gender affects changes in carotid wall vibrations and identifies the most effective image-tracking method, which was found to be the Gunnar-Farneback method. While no algorithm was found to be superior, the Gunnar-Farneback method generally performed better. The results indicate that vibration

Table 4. Comparison between previous papers and our results

Row	Researchers	Method	P-value	r-squared	Correlation
1	Zahn <i>et al.</i> in 2011	Optical flow	< 0.001		
2	Yousefi <i>et al.</i> in 2014	Peak-to-peak distance vibrations	< 0.001(age) < 0.001(BMI)	$r = -0.5456$ $r = -0.5821$	
3	Gao <i>et al.</i> in 2018	Tracing method based on nonlinear space	< 0.001		≥ 0.9948 for longitudinal ≥ 0.9966 for radial
4	Our paper	Optical flow, Gunnar-Farneback method	< 0.001	$r = -0.4590$ $r = -0.6510$	$Corr = -0.6770$

decreases with increasing age and BMI, as seen in the negative gradient of the graph.

Acknowledgments

The authors acknowledge the biomedical engineering department of the Islamic Azad University (Science and Research Branch) for providing the ultrasound device for data acquisition.

This article contains studies with human participants and the ethical code is [IR.IAU.SRB.REC.1398.090].

The authors declare that they have no conflicts of interest.

This research received no specific grant from any funding agency in the public, commercial or not-for-profit sectors.

References

- 1- Z. Gao *et al.*, "Motion Tracking of the Carotid Artery Wall From Ultrasound Image Sequences: a Nonlinear State-Space Approach." *IEEE Trans Med Imaging*, Vol. 37 (No. 1), pp. 273-83, Jan (2018).
- 2- A. Tokita *et al.*, "Carotid arterial elasticity is a sensitive atherosclerosis value reflecting visceral fat accumulation in obese subjects." *Atherosclerosis*, Vol. 206 (No. 1), pp. 168-72, Sep (2009).
- 3- I. A. Hein and W. R. O'Brien, "Current time-domain methods for assessing tissue motion by analysis from reflected ultrasound echoes-a review." *IEEE Trans Ultrason Ferroelectr Freq Control*, Vol. 40 (No. 2), pp. 84-102, (1993).
- 4- Xiaoliang Gong and Stephan Bansmer, "Horn-Schunck optical flow applied to deformation measurement of a birdlike airfoil." *Chinese Journal of Aeronautics*, Vol. 28 (No. 5), pp. 1305-15, (2015).
- 5- Andrés Bruhn, Joachim Weickert, and Christoph Schnörr, "Combining the Advantages of Local and Global Optic Flow Methods." in *Pattern Recognition (Lecture Notes in Computer Science)*, (2002), pp. 454-62.
- 6- Q. Tao, Y. Wang, P. Fish, W. Wang, and J. Cardoso, "The wall signal removal in Doppler ultrasound systems based on recursive PCA." *Ultrasound Med Biol*, Vol. 30 (No. 3), pp. 369-79, Mar (2004).
- 7- D. Boukerroui, J. A. Noble, and M. Brady, "Velocity estimation in ultrasound images: a block matching approach." *Inf Process Med Imaging*, Vol. 18pp. 586-98, Jul (2003).
- 8- M. Cinthio, A. R. Ahlgren, T. Jansson, A. Eriksson, H. W. Persson, and K. Lindstrom, "Evaluation of an ultrasonic echo-tracking method for measurements of arterial wall movements in two dimensions." *IEEE Trans Ultrason Ferroelectr Freq Control*, Vol. 52 (No. 8), pp. 1300-11, Aug (2005).
- 9- M. Cinthio, H. Hasegawa, and H. Kanai, "Initial phantom validation of minute roughness measurement using phase tracking for arterial wall diagnosis non-invasively in vivo." *IEEE Trans Ultrason Ferroelectr Freq Control*, Vol. 58 (No. 4), pp. 853-7, Apr (2011).
- 10- A. Gastouniotti, S. Golemati, J. S. Stoitsis, and K. S. Nikita, "Carotid artery wall motion analysis from B-mode ultrasound using adaptive block matching: in silico evaluation and in vivo application." *Phys Med Biol*, Vol. 58 (No. 24), pp. 8647-61, Dec 21 (2013).
- 11- G. Zahnd *et al.*, "Measurement of two-dimensional movement parameters of the carotid artery wall for early detection of arteriosclerosis: a preliminary clinical study." *Ultrasound Med Biol*, Vol. 37 (No. 9), pp. 1421-9, Sep (2011).
- 12- G. Zahnd, M. Orkisz, A. Serusclat, P. Moulin, and D. Vray, "Evaluation of a Kalman-based block matching method to assess the bi-dimensional motion of the carotid artery wall in B-mode ultrasound sequences." *Med Image Anal*, Vol. 17 (No. 5), pp. 573-85, Jul (2013).
- 13- G. Zahnd, S. Salles, H. Liebgott, D. Vray, A. Serusclat, and P. Moulin, "Real-time ultrasound-tagging to track the 2D motion of the common carotid artery wall in vivo." *Med Phys*, Vol. 42 (No. 2), pp. 820-30, Feb (2015).
- 14- G. Zahnd, K. Saito, K. Nagatsuka, Y. Otake, and Y. Sato, "Dynamic Block Matching to assess the longitudinal component of the dense motion field of the carotid artery wall in B-mode ultrasound sequences - Association with coronary artery disease." *Med Phys*, Vol. 45 (No. 11), pp. 5041-53, Nov (2018).
- 15- F. Yousefi Rizi, S. K. Setarehdan, H. Behnam, and Z. Alizadeh Sani, "Study of the effects of age and body mass index on the carotid wall vibration: extraction methodology and analysis." *Proc Inst Mech Eng H*, Vol. 228 (No. 7), pp. 714-29, Jul (2014).
- 16- Spyretta Golemati, Aimilia Gastouniotti, and Konstantina S. Nikita, "Ultrasound-Image-Based Cardiovascular Tissue Motion Estimation." *IEEE Reviews in Biomedical Engineering*, Vol. 9pp. 208-18, (2016).
- 17- B. I. Chuang, J. H. Hsu, L. C. Kuo, I. M. Jou, F. C. Su, and Y. N. Sun, "Tendon-motion tracking in an ultrasound image sequence using optical-flow-based block matching." *Biomed Eng Online*, Vol. 16 (No. 1), p. 47, Apr 20 (2017).
- 18- Deqing Sun, Stefan Roth, and Michael J. Black, "Secrets of optical flow estimation and their principles." Presented at the *2010 IEEE Computer Society Conference on Computer Vision and Pattern Recognition*, (2010).

- 19- M. Larsson, F. Kremer, P. Claus, T. Kuznetsova, L. A. Brodin, and J. D'Hooge, "Ultrasound-based radial and longitudinal strain estimation of the carotid artery: a feasibility study." *IEEE Trans Ultrason Ferroelectr Freq Control*, Vol. 58 (No. 10), pp. 2244-51, Oct (2011).
- 20- L. E. Tarnec L, F. Destrempes, G. Cloutier, and D. Garcia, "A Proof of Convergence of the Horn and Schunck Optical Flow Algorithm in Arbitrary Dimension." *SIAM J Imaging Sci*, Vol. 7 (No. 1), pp. 277-93, (2014).
- 21- M. J. Black and P. Anandan., "A framework for the robust estimation of optical flow. In Computer Vision." *Fourth International Conference* pp. 231–36, (1993).
- 22- Andrés et al. Bruhn, "'Lucas/Kanade Meets Horn/Schunck: Combining Local and Global Optic Flow Methods.'" *International Journal of Computer Vision 61 (2004)*, pp. 211-31, (2021).
- 23- Nidhal Azawi, "Adaptive Motion Compensated Spatial Temporal Filter of Colonoscopy Video." *Iraqi Journal of Science*, pp. 4148-57, (2021).
- 24- Steve Beuve, Samuel Callé, Elise Khoury, Emmanuel Gilles Simon, and Jean-Pierre Remenieras, "Natural shear wave imaging using vocal tract vibrations: Introducing vocal passive elastography (V-PE) to thyroid elasticity mapping." *Applied Physics Letters*, Vol. 118 (No. 2), (2021).
- 25- L. Saba et al., "Multimodality carotid plaque tissue characterization and classification in the artificial intelligence paradigm: a narrative review for stroke application." *Ann Transl Med*, Vol. 9 (No. 14), p. 1206, Jul (2021).
- 26- J. M. Rothberg et al., "Ultrasound-on-chip platform for medical imaging, analysis, and collective intelligence." *Proc Natl Acad Sci U S A*, Vol. 118 (No. 27), Jul 6 (2021).
- 27- Eleanor C. Mackle, Joanna M. Coote, Elizabeth Carr, Callum D. Little, Gijs van Soest, and Adrien E. Desjardins, "Fibre optic intravascular measurements of blood flow: A review." *Sensors and Actuators A: Physical*, Vol. 332(2021).
- 28- A. Babbar, V. Jain, D. Gupta, and D. Agrawal, "Histological evaluation of thermal damage to Osteocytes: A comparative study of conventional and ultrasonic-assisted bone grinding." *Med Eng Phys*, Vol. 90pp. 1-8, Apr (2021).
- 29- S. Iskander-Rizk et al., "Micro Spectroscopic Photoacoustic (musPA) imaging of advanced carotid atherosclerosis." *Photoacoustics*, Vol. 22p. 100261, Jun (2021).
- 30- D. Lopes et al., "Analysis of finite element and finite volume methods for fluid-structure interaction simulation of blood flow in a real stenosed artery." *International Journal of Mechanical Sciences*, Vol. 207(2021).